International Symposium on Hydraulic Structures

Jun 29th, 4:00 PM - 6:00 PM

Optimizing A New Flow Diversion Structure For The Planned Expanding Of The Spillway For The Malter Dam In Germany Using A Physical Hydraulic Model

J. Schmidt
University of Siegen, jessica.schmidt@uni-siegen.de

J. Wieland
University of Siegen

J. Jensen
University of Sigen

Recommended Citation

Schmidt, J., Wieland, J., Jensen, J. (2016). Optimizing A New Flow Diversion Structure For The Planned Expanding Of The Spillway For The Malter Dam In Germany Using A Physical Hydraulic Model. In B. Crookston & B. Tullis (Eds.), Hydraulic Structures and Water System Management. 6th IAHR International Symposium on Hydraulic Structures, Portland, OR, 27-30 June (pp. 387-396). (ISBN 978-1-884575-75-4).

6th International Symposium on Hydraulic Structures Portland, Oregon, USA, 27-30 June 2016
Hydraulic Structures and Water System Management
ISBN 978-1-884575-75-4 DOI: 10.15142/T3220628160853

Optimizing A New Flow Diversion Structure For The Planned Expanding Of The Spillway For The Malter Dam In Germany Using A Physical Hydraulic Model

J. Schmidt[1], J. Wieland[1] and J. Jensen[1]
[1]Research Institute for Water and Environment (fwu)
University of Siegen
Paul-Bonatz-Str. 9-11
57076 Siegen
Germany
E-mail: jessica.schmidt@uni-siegen.de

ABSTRACT

The State Reservoir Administration of Saxony is planning to expand the spillway discharge capacity of the 102-year-old Malter Dam. After a catastrophic flood in 2002, updated hydrologic modeling indicated that the design discharges for the dam had increased significantly. As a result, the original spillway discharge capacity was insufficient to pass the revised design flows. A design concept was developed to add a second spillway and stilling basin to the dam, and to pass flow into this spillway using a novel vertical flow separator. The design and performance of this system was evaluated using a 1:25-scale physical model. The modeling activities were performed by the Research Institute for Water and Environment located at the University of Siegen. The modeling effort led to an improved design of the vertical flow separator, which meets the needs of the project and will allow for an increase in the spillway discharge capacity to satisfy dam safety concerns.

Keywords: *diversion structure, physical modeling, spillway, dam, flood safety*

1. INTRODUCTION

The State Reservoir Administration of Saxony (LTV) is planning to expand the spillway of the 102 year old Malter Dam. This is necessary to reinstate the flooding safety of the dam, which has currently not been given due to an adaptation of the hydrological design discharges. As part of this project, the LTV commissioned the Research Institute Water and Environment (fwu) of the University of Siegen to perform a hydraulic model test for review and optimization of the hydraulic functionality.

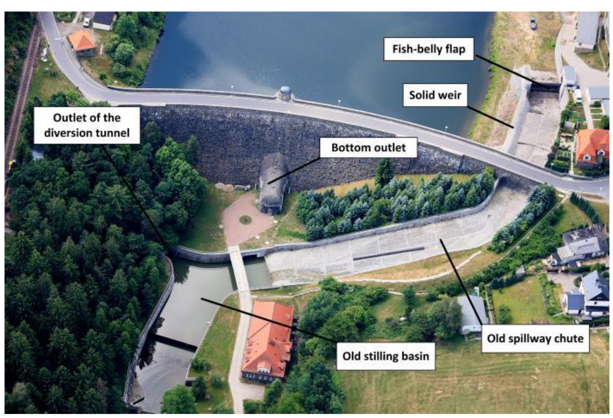

Figure 1. Aerial view of the Malter Dam in 2008 (Source: LTV)

The Malter Dam was built from 1908 to 1913 in the valley of the river "Rote Weißeritz" and has a storage volume of 8.78 million m³. The 193 m long curved dam consists of quarry stone masonry. The dam serves mainly for flood protection, as well as for recreational activities and industrial water supply. Furthermore, an annual average of 1.7 million kWh of electricity from hydropower is gained at the Malter Dam. In normal operation, the water of the dam is released through the bottom outlet (two pipelines, each with DN 1,000) of the dam into the riverbed. If a flood is expected, the 200 m long diversion tunnel by the right side of the slope can be used for pre-release. In case of floods, the flow discharges through the spillway, which lies on the left side of the slope in the form of a fish-belly flap that is arranged laterally to a masonry weir with an overflow threshold, through the wall passage over the old spillway chute, and down to the old stilling basin below the dam (Figure 1).

The extreme flood event in August 2002 resulted in damage and overloading of the spillway of the Malter Dam, causing extensive flooding at the lower reaches of the "Rote Weißeritz". The flood also lead to huge damages in Dresden at the Elbe river, which is only about 20 km away from the Malter Dam. The total damage of the flood event in Germany amounted to about 10 billion euros. The extreme flood event at the Malter Dam is shown in Figure 2. On the left side is the view from the dam into the old spillway chute. On the right side is the view from the dam to the fish-belly flap and the masonry weir.

Figure 2. Extreme flood event at the Malter Dam in 2002 (Source: LTV)

In 2006, new design discharges were determined on the basis of new rainfall-runoff models. The comparison of the last design discharges of the Malter Dam in 1983 and of the new design discharges in 2014 show that the design discharges have increased about 131% for the flood discharge $HQ_{1,000}$ (= BHQ_1 = design flood event, that statistically occurs every 1,000-years) from 125 m³/s to 289 m³/s and about 137% for the flood discharge $HQ_{10,000}$ (= BHQ_2 = design flood event, that statistically occurs every 10,000-years) from 166 m³/s to 393 m³/s. The spillway of the Malter Dam was not originally designed for these increased design discharges. Therefore, the flooding safety of the Malter Dam is no longer guaranteed. For this reason, the LTV is currently planning the expansion of the spillway to restore the flood safety the Malter Dam.

Figure 3. Spillway of the Malter Dam 2014 (left) (Source: LTV); Evened bottom slope in the hydraulic model (right)

As part of the development plans, the expansion of the existing spillway with an additional spillway chute with a new stilling basin has turned out to be the preferred option for an economically viable capacity improvement of the spillway. The expansion of the spillway also includes a lowering of the sole of the wall passage to about 1.5 m with a bed slope of 3.5 % to prevent over-fill (Figure 3). The application of the two spillways occurs behind the wall passage by a new kind of flow diversion structure with a vertical flow separation. Furthermore, the hydraulic performance of the diversion tunnel is increased by replacing the existing slide valves with more efficient slide valves (3 x 2 slide valves in two levels in closed type w/h = 1,000/1,000 mm). Due to the mutual flow influence of the individual components and complex geometries, for which no hydraulic boundary conditions or calibration measurements are presently available, a physical hydraulic model test was required (Kobus 1980).

2. HYDRAULIC MODEL TEST

2.1. Model Features and Measuring Technique

The hydraulic model (1:25) of the Malter Dam was built due to the dominant gravity and inertial force as a Froude model and includes a part of the water storage area, the dam, the existing spillway, the planned expansion of the spillway (diversion structure, new spillway chute, new stilling basin), the bottom outlet, the diversion tunnel, the old stilling basin, and a part of the below lying river, “Rote Weißeritz” (Figure 4). The model extends over a length of 19.60 m, with a maximum width of 7.20 m within an area of 85 m². The water area of the storage space in the model comprises about 22 m²; the storage volume in a flood event is about 14 m³. The largest hydraulic height difference ranges about 1.58 m. The hydraulic model has been designed with a concrete surface.

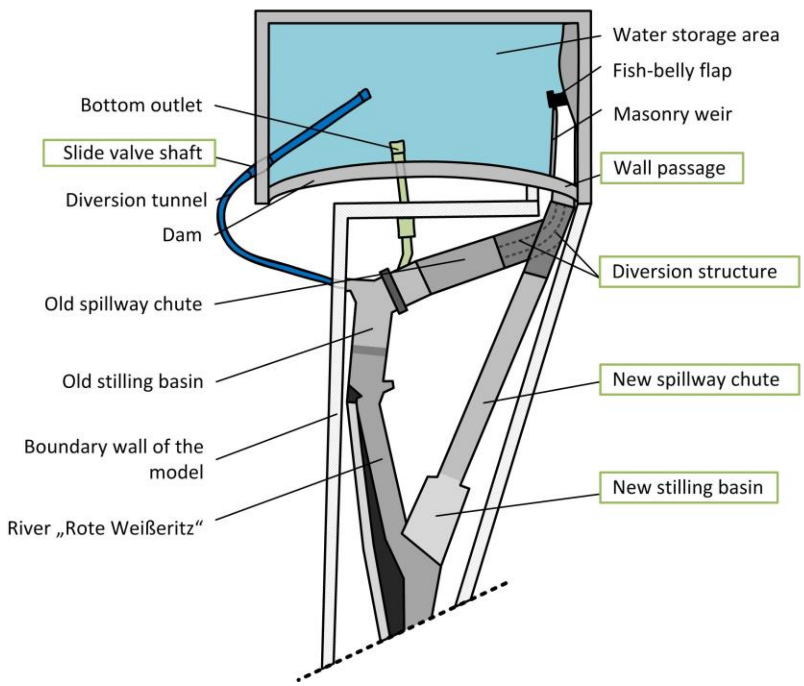

Figure 4. Schematic sketch of the hydraulic model of the Malter Dam; outlined in green are the components that are newly built or rebuilt in the context of the expansion

The control of the outflow amount, the settings of the valves (2 x bottom outlet, 3 x diversion tunnel, 1 x fish-belly flap), and the setting of the lower water level at the end of the model was performed fully automatic and computer controlled by servomotors that achieve a positioning accuracy of 0.1 mm. The inflow into the model was measured by an inductive flowmeter (IDM) in the supply line, whereby the accuracy of the discharge measurement was achieved within 0.1% of full scale. The maximum load to be examined in nature PMF (= probable maximum flood = HQ_{max}) = 461 m³/s has been examined as an inflow of PMF = 147.5 l/s in the model. For the investigations, the water level was recorded at six positions with ultrasound measuring probes in real-time. These data were supplemented and densified by further measured water levels and velocity profiles. Furthermore, differential pressure measurements were performed for qualitative statements, and video and image materials were recorded. With the used measurement technology, highly precise measurements and an optimum reproducibility of the measurement results were guaranteed.

2.2. Optimization and Investigation Aspects

Special optimization and examination aspects in the model test included the outflow distribution into the diversion structure, the hydraulic performance of the new spillway chute, the dimensions of the new stilling basin, and the impact of the planned increase in the hydraulic performance of the diversion tunnel with simultaneous operation of the spillway. To optimally utilize the existing building stock and to prevent overloading of the existing spillway, the flow behavior in the diversion structure was analyzed to optimize the loading of the two spillways. In the hydraulic model test, seven load cases (HQ_{80}, HQ_{100}, HQ_{200}, HQ_{500}, $HQ_{1,000}$, $HQ_{10,000}$ and PMF) of HQ_{80} = 36.8 m³/s to PMF = 461 m³/s with the respective settings of the operating facilities (1 to 2 opened slide valves of the bottom outlet, 1 to 3 opened slide valves of the diversion tunnel, upper edge of the fish-belly flap from 333.0 to 330.5 mNN) were examined. According to the investigation concept, all objects of study have been investigated for the planned state (Jensen et al. 2015). Since individual conversion measures, in turn, have effects on the entire outflow behavior of the model experiment, the hydraulic model was rebuilt from the plan state to optimization state (optimized end state) using the recommended conversion measures; subsequently, all the objects of the investigation were examined again.

A particular challenge is the hydraulic performance and the optimization of the outflow process in both closed and curved components diversion tunnel and diversion structure, because of the supercritical flow and complex transitions from free-surface to pressure drain in conjunction with air entry (Schmidt et al. 2015a). In addition, the outflow processes in the diversion tunnel and in the diversion structure depend decisively on the boundary conditions above and below.

3. INVESTIGATIONS OF THE DIVERSION STRUCTURE IN THE MODEL TEST

3.1. Proof of the Functional Principle of the Diversion Structure (Planned Geometry)

Behind the wall passage, the construction of a transition channel is planned, which leads to the diversion structure. On the upper level, the new spillway chute and stilling basin are connected. In the case of a flood, the runoff is first discharged through an opening in the sole of the diversion structure on the lower level into the old spillway chute (Figure 5, left). Due to the optimal design, the hydraulic efficiency of the opening and of the old stilling basin should correspond, taking into account inflows into the stilling basin from the bottom outlet and diversion tunnel, preventing an overloading of the old stilling basin. When the flood discharge exceeds the hydraulic performance of the opening, and thus of the old stilling basin, there is an overflowing of the opening and the remaining flood discharge is passed onto the upper level of the diversion structure into the new spillway chute (Figure 5, right).

The functionality of the planned diversion structure could be demonstrated in a first-test series. However, there was a splashing phenomenon from the sole opening to the upper level into the new spillway chute whereby the uneven inflow of new spillway chute and the associated cross wave formation were amplified (Figure 6, left). Even at the old spillway chute, a cross wave formation could be observed. But this resulted from the supercritical flow through the three curved channels of the diversion structure below the sole opening (Figure 7, left). The optimization of the cross waves was subordinate to the overarching goal of safe dissipation of the flood runoff (Schmidt et al. 2015a).

Due to the increased efficiency of the diversion tunnel by the new valves in the slide valve shaft and through the operational recommendations by Jensen et al. (2015) for operation without ventilation in pressure drain, the old stilling basin was overloaded in the design load cases $HQ_{1,000}$ and $HQ_{10,000}$ in the planned state. To avoid this, several geometries and the opening width of the vertical separator were investigated and optimized in five experimental test series. For these tests, discharge and pressure measurements, as well as video and image recordings, were used.

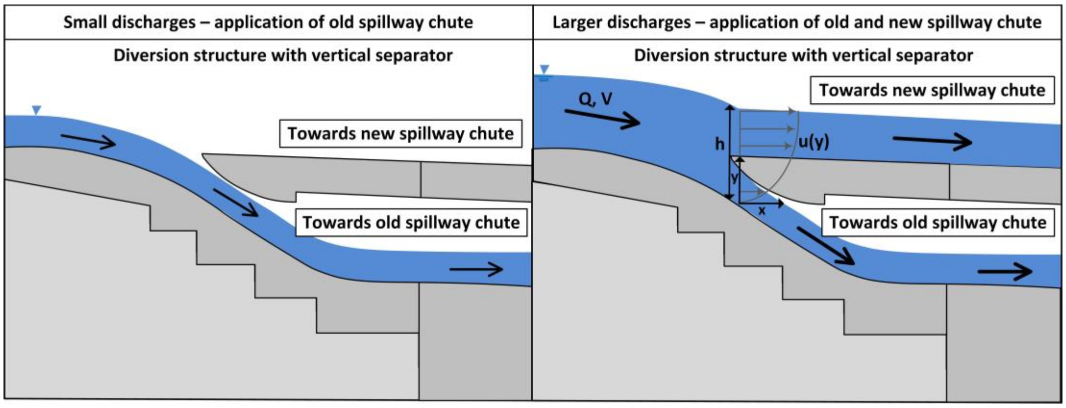

Figure 5. Functional principle of the diversion structure during smaller and larger outflows

Figure 6. Comparison of the splashing effect in experiment series 4 and 5 (optimized geometry), Q = 100 m³/s

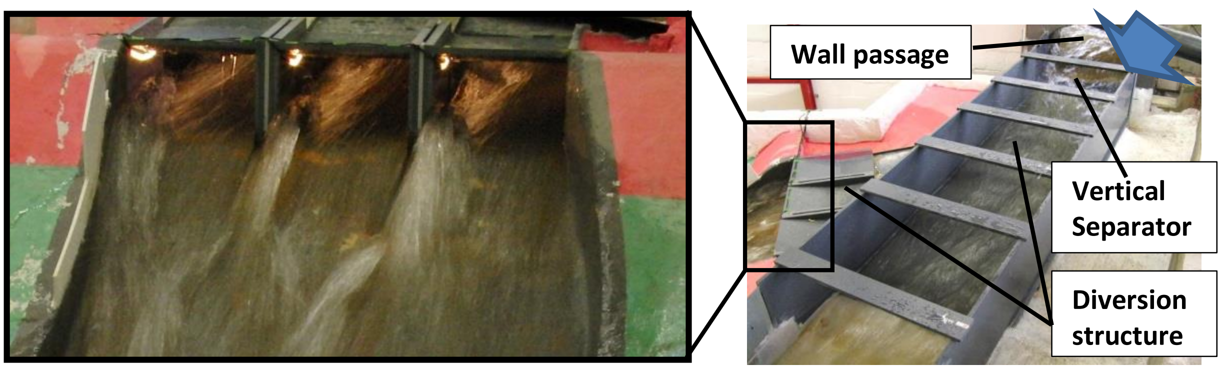

Figure 7. View into the three channels of the lower diversion structure (left) and at the upper diversion structure (right) in the optimized state in the hydraulic model, load case $HQ_{1,000}$

3.2. Optimization of the Vertical Separator Geometry (experiment series 1 to 5)

According to the investigations of the plan state (experiment series 1), first the partial discharge into the old spillway chute should be reduced by shifting the vertical separator horizontally to shrink the opening width from 0.80 m to 0.64 m (experiment series 2). Due to the uneven flow in the wall passage in the planned state, the discharge flows unevenly over the vertical separator, and, hence, the new spillway chute is unevenly applied so that cross waves arise. This negative effect was even stronger in experiment series 2 because the lowered surface curve collides with the edge of the vertical separator. To optimize this issue, the rounding of the vertical separator was adjusted in experiment series 3 so that the inlet gap again corresponds approximately to the original length of the planned geometry (3.17 m). The reduction of the opening of the vertical separator (0.64 m) has been preserved. It became apparent that this geometry leads to an increased splashing effect. To avoid the splashing effect, the vertical separator was adjusted in experiment series 4 so that the edge is more pointed. But in experiment series 4, the splashing effect was considerably strengthened (Figure 6, left). Based on these observations, was concluded that the splashing effect is not due to the collision of the water with the edge of the vertical separator.

The splashing phenomenon could be explained after four extensive experiment series: Due to the larger opening of the inlet gap of the vertical separator compared to the control section below, more water is discharged as the control section of the vertical separator can absorb under the given pressure conditions. In the vicinity of the expansion behind the control section, a negative pressure temporarily occurs in the area of the control section, so additional runoff is pressed in the diversion structure by the atmospheric air pressure. This increases the performance of the diversion structure but also the risk of cavitation. The rounding of the vertical separator is therefore not necessary, and even a hindrance, as the water jet is in contact with the rounding of the vertical separator and the cross-section, which adjusts pressure drain, is increased. To avoid the negative impact of the rounded vertical separator, an optimization geometry in wedge shape was constructed and examined in experiment series 5 (Schmidt et al. 2015b). Deviating to the planned geometry, the control section was set without rounding directly into the inlet gap of the vertical separator (Figure 8, right).

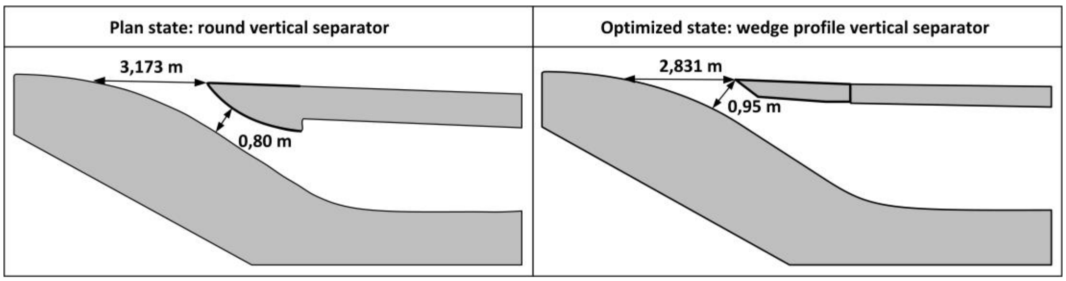

Figure 8. Schematic sketch of the geometry of the vertical separator in the plan state (left) and in the optimized state (right), longitudinal section

The flow now breaks off directly at the wedged edge control section so that the discharge is no longer in contact with the vertical separator and no pressure drain in this field may develop anymore. The runoff is now discharged below the vertical separator completely as free surface discharge, and there is no splashing effect at the inlet gap. Due to the free surface discharge, the flow velocity in the three curved channels is lower than in the state plan. Therefore, the water level deflection is smaller, the discharge flows more uniformly into the old spillway chute, and the expression of the cross waves is reduced. An utter prevention of cross wave formation is impossible due to the geometry of the diversion structure and of the old spillway chute (Schmidt et al. 2015a). Nevertheless, the new geometry of the vertical separator, as can be seen in Figure 9, generates an even more equal diversion of the flow. Due to the narrow design of the vertical separator, generous underwater ventilation is ensured and the structural complexity is significantly reduced. The risk of cavitation in the area of deduction is now minimal.

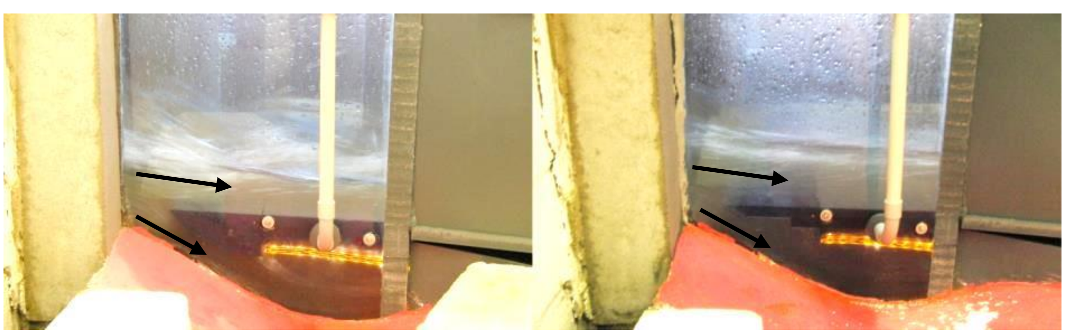

Figure 9. Geometry of the vertical separator in the planned state (left) and in the optimized state (right) in the hydraulic model, load case $HQ_{1,000}$

4. NUMERICAL INVESTIGATIONS OF THE OPTIMIZED DIVERSION STRUCTURE

For the numerical description of the discharge partition by the diversion structure, additional measurements of the water level h (Figure 5) at the edge of the vertical separator for 12 outflows (Q = 50, 60, 70, 80, 90, 100, 110, 120, 130, 140, 150 and 200 m³/s) were recorded. From the measured data, the mean water level h, the mean water level under the vertical separator y (Figure 5), and the mean velocity in the whole flow cross-section V (Figure 5) were determined for each load case. To calculate the mean velocity under the vertical separator $u_{mean,lo}$ and thereby the partial discharges into the old and the new spillway chute, the velocity profiles and the shear stress distribution were determined both for the simplified consideration of a predominantly two-dimensional flow and the three-dimensional flow of the measured partial discharges in the hydraulic model.

4.1. Simplified Consideration as a Predominantly Two-Dimensional Flow

Due to the change in slope behind the wall passage into the diversion structure, there is a non-uniform channel flow. Jirka and Lang (2009) say that local speed profiles of non-uniform channel flow are in a first approximation, similar to those in uniform flow. So for open channel flow with a large width ($w >> h$) and a small bed slope, a linear shear stress distribution may approximatively be assumed. The maximum shear stress at the sole τ_0 (y = 0) is described as

$$\tau_0 = \gamma \cdot I_0 \cdot h = \rho \cdot g \cdot I_0 \cdot h \tag{1}$$

where ρ is the density of water (1,000 kg/m³), g is the constant of gravitation (9.81 m/s²), I_0 is the bottom slope, and h is the water level. The shear stress is in kinematic form, expressed as the shear stress velocity or friction velocity u_*.

$$u_* = \sqrt{\frac{\tau_0}{\rho}} \tag{2}$$

From the measured values of the water depth h at the edge of the vertical separator, the turbulence parameter u_*/V was determined for each load case and shown in Figure 11 (red line). The values range from 0.125 to 0.168 and, thus, lie all in the rough area. Also, the Reynolds number confirms that it is a fully rough open channel flow (100 > Re) (Chanson 2004). The current flow is characterized by turbulent momentum exchange operations in the form of fluctuating vortex motions, which are superposed on the mean velocity profile $u(y)$. These internal turbulence mechanisms control the shape of the resulting velocity profile $u(y)$ because the logarithmic velocity profile results from the friction velocity and depends on the sole roughness k_s. The turbulent channel flow corresponds to a boundary layer flow that is over the entire water depth fully developed. For turbulent flows with a fixed boundary, the logarithmic law of the velocity distribution is applicable (Jirka and Lang 2009, Chaudhry 2008):

$$\frac{u}{u_*} = \frac{1}{\kappa} \cdot ln(y) + C \tag{3}$$

where κ is the Karman constant Kappa (≅ 0.40), C is a function of the boundary conditions of the respective flow subzone, y is the partial water depth in which the velocity is to be determined, and u is the velocity at the water depth y. The simplified velocity profile can be represented dimensionless (normalized) by the mean velocity in the main flow direction V (Jirka and Lang 2009).

$$\frac{u}{V} = 1 + 2.5 \cdot \frac{u_*}{V} \cdot \left(1 + ln\frac{y}{h}\right) <=> u = V \cdot \left(1 + 2.5 \cdot \frac{u_*}{V} \cdot \left(1 + ln\frac{y}{h}\right)\right) \tag{4}$$

Eq. (4) shows the dependence of the velocity profile of the turbulence parameter u_*/V, which is a measure for the out of the frictional resistance arising turbulent vortex motions. The velocity profiles at the vertical separator could be determined as a function of y/h (= 0.05 to 1.0) from the turbulence parameters u_*/V and the mean velocities in the whole flow cross-section V, calculated from the measured. Figure 12 (left) shows the velocity profiles for each load case. The velocity u at the water level under the vertical separator y is also marked. For each load case, the integral over the curve up to the measured value of y/h has been calculated, and by the mean value theorem of the integral calculus, the mean velocity of the partial discharge under the vertical separator $u_{mean,\, lo}$ has been determined (Eq. (5)). The mean velocity above the vertical separator has been determined correspondingly. From the mean velocities above and below the vertical separator, the partial discharges into the old and the new spillway chute could be calculated using the continuity equation.

$$u_{mean,lo} = \frac{1}{\frac{y}{h}-0.05} \cdot \int_{0.05}^{y/h} \left(V \cdot \left(1 + 2.5 \cdot \frac{u_*}{V} \cdot \left(1 + ln\frac{y}{h} \right) \right) \right) \tag{5}$$

Figure 10 shows the comparison of the calculated and the in the model test measured partial discharges in the old and the new spillway chute. The calculated partial discharges show a good agreement to the measured discharges for the load cases Q = 50 and 60 m³/s when the discharge flows completely under the vertical separator in the old spillway chute. But for all other load cases, there are very high differences. A possible reason is the assumption of a linear shear stress distribution in the turbulent flow when the flow is divided into the old and new spillway chutes. Thus, the simplified assumption of a predominantly two-dimensional flow before the division structure is not effective for these load cases. A mere numerical calculation of the partial discharges with this approach is not possible. The three-dimensionality of the flow has to be considered, which is why a hydraulic model test for determining the partial outflows is imperative.

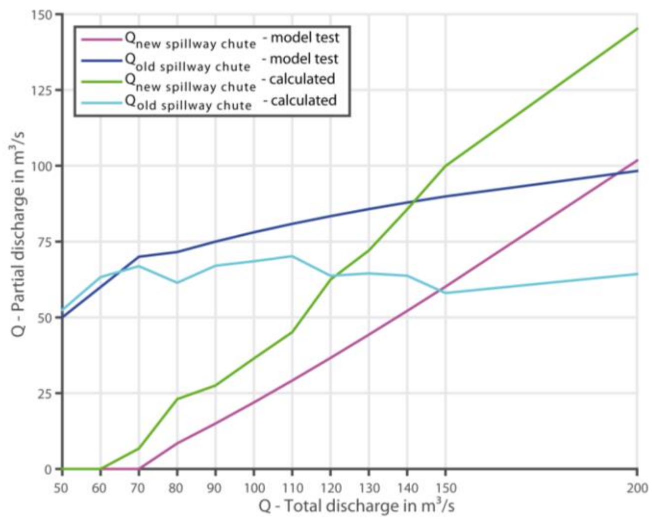

Figure 10. Partial discharges on the old and the new spillway chute (calculated and measured in the model test)

4.2. Three-Dimensional Flow of the Measured Partial Discharges

According to Bollrich (2013), the shear stress due to turbulence results from the product of the density with the temporal mean value of the product of the velocity fluctuation components in flow direction v_s' and transverse v_n'.

$$\tau = \rho \cdot \overline{v_s' \cdot v_n'} \tag{6}$$

Accordingly, the shear stress velocity results to

$$u_* = \sqrt{\frac{\tau}{\rho}} = \sqrt{\overline{v_s' \cdot v_n'}} \tag{7}$$

The shear stress due to turbulence is thus proportional to the square of a velocity.

$$\tau = \rho \cdot u_*^2 \tag{8}$$

From the partial discharges measured in the model test, a formula for the partial discharge below the vertical separator $Q_{old\ spillway\ chute}$ could be determined, valid for the total discharges Q_{total} > 70 m³/s (Figure 10).

$$Q_{old\ spillway\ chute} = 29.158 \cdot ln(Q_{total}) - 56.213 \tag{9}$$

For $Q_{total} \leq 70$ m³/s applies $Q_{total} = Q_{old\ spillway\ chute}$ because up to this discharge, the whole discharge is drained under the vertical separator into the old spillway chute. With the calculated partial discharges $Q_{old\ spillway\ chute}$ and the continuity equation (Eq. (10)), the mean velocity under the vertical separator u was determined.

$$u = \frac{Q_{old\ spillway\ chute}}{w \cdot y} \tag{10}$$

The shear stress velocity u_* was calculated with Eq. (4) dissolved to u_*, and the shear stress due to turbulence was calculated with Eq. (8). The turbulence parameter u_*/V calculated from Eq. (2) (red) and from Eq. (4) (blue) are shown in Figure 11. The blue line shows that the shear stress velocity cannot be calculated for $h \leq 1$, because the shear stress velocity is then zero (e.g. $h = y = 0.87$ for $Q = 50$ m³/s and $h = y = 1.05$ for $Q = 60$ m³/s).

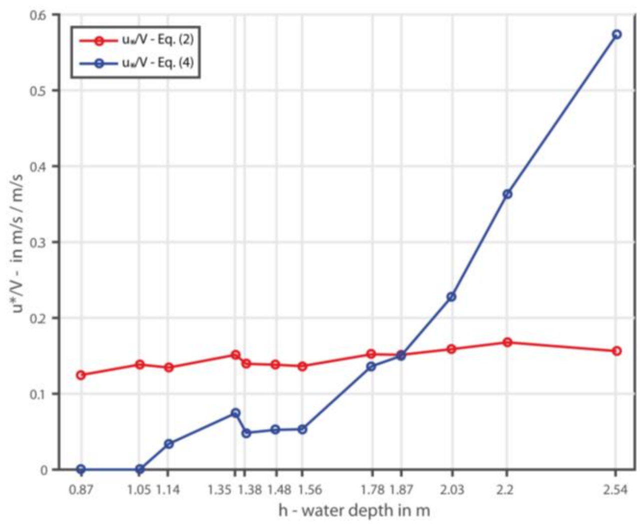

Figure 11. Turbulence parameter u_*/V for the measured water depth at the vertical separator of the diversion structure for the load cases $Q = 50$ to 200 m³/s calculated from Eq. (2) (red) and Eq. (4) (blue)

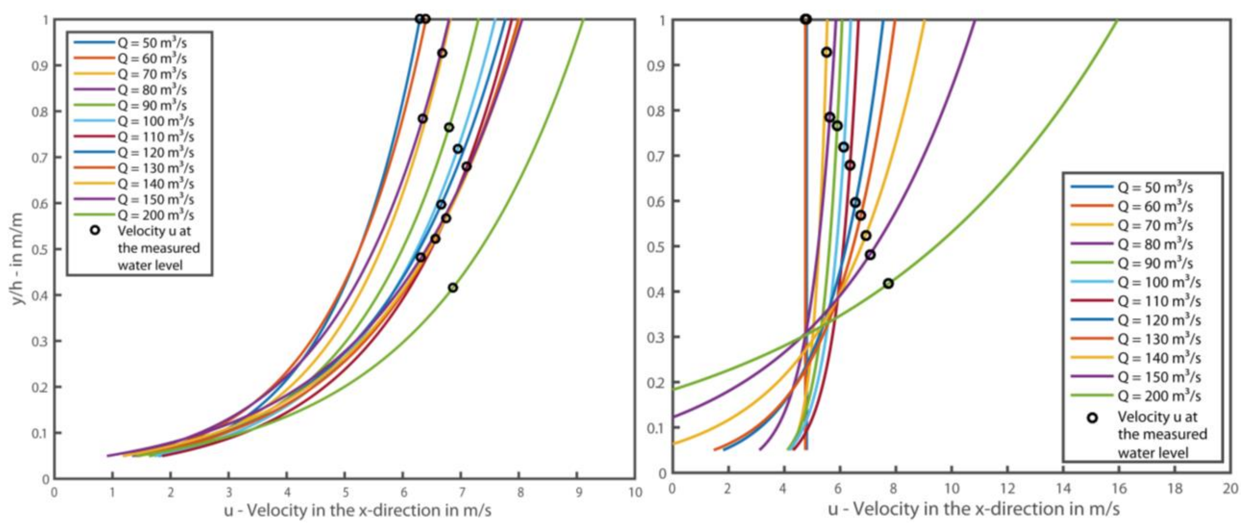

Figure 12. Velocity profiles as a function of y/h, load cases $Q = 50$ to 200 m³/s, Left: 2-D flow, Right: 3-D flow

The shear stress velocity u_* used in Eq. (4) yield to the velocity distributions for each load case, shown in Figure 12, right. These velocity distributions consequently result for the measured partial discharges. Again, it can be seen that this method is not applicable for $h \leq 1$ ($Q = 50$ and 60 m³/s).

5. CONCLUSION

With the hydraulic model test for the Malter Dam, the hydraulic performance and reliability of the preliminary draft were examined, optimized, and verified. The planned geometry of the vertical separator of the diversion structure was rounded with a control section lying below the opening. However, the studies on the planning geometry showed heterogeneous hydraulic phenomena. A vacuum formed in the area of the control section, which led to an increased risk of cavitation, an accelerated outflow with suction effect, and a splashing effect from the vertical separator in the above located new spillway chute. The rounding of the vertical separator, on which the discharge was abutted, was finally removed, and the vertical separator could be adjusted to a wedge shape. The control section is now lying directly in the sole opening. The discharge in the lower diversion structure now flows with a completely free surface. Vacuum and the associated negative hydraulic consequences no longer occur with the optimized geometry of the vertical separator in a wedge shape. As another side effect, the uneven inflow over the vertical separator into the new spillway chute is now more even because of the prevented splashing effect, whereby, the cross waves on the new spillway chute have been considerably reduced. In this contribution, it was also shown that numerical calculations of the partial discharges in the diversion structure using the simplified assumption of a two-dimensional flow are not effective, and, thus, a hydraulic model test is essential for the safe design of the diversion structure.

The challenge of enlargement of the spillway of the Malter Dam consisted primarily in making optimum use of the existing building stock so that overloading of the old spillway is excluded. By using the hydraulic model test, reliable statements on the runoff process for a worldwide new diversion structure could be made. As a result, the division structure was optimized so that the operational reliability and hydraulic efficiency, even in extreme flood events (PMF), is ensured. Thus, a safe and economic design could be achieved with this hydraulic model test.

6. ACKNOWLEDGMENTS

This work was funded by the State Reservoir Administration of Saxony (LTV). Special thanks to Dipl.-Ing. Bernd Findeisen from the LTV and Dr.-Ing. Holger Haufe from the Lahmeyer Hydroproject GmbH, for their valuable support and their constructive recommendations on this project.

7. REFERENCES

Bollrich, G. (2013). Technische Hydromechanik 1. 7th Edition, Beuth Verlag GmbH, Berlin, Germany, 2013.

Chanson, H. (2004). The Hydraulics of Open Channel Flow: An Introduction. 2nd Edition, Elsevier, Oxford, Great Britain, 2004.

Chaudry, H. (2008). Open-Channel Flow. 2nd Edition, Springer Science+Business Media, New York, USA, 2008.

Jensen, J., Schmidt, J., and Wieland, J. (2015). Endbericht. Hydraulischer Modellversuch zum Projekt „Talsperre Malter – Erweiterung der Hochwasserentlastungsanlage“. Unpublished project final report. University of Siegen, Germany, 6th July 2015.

Jirka, G. H., and Lang, C. (2009). Einführung in die Gerinnehydraulik. 2nd Edition, Universitätsverlag Karlsruhe, Karlsruhe, Germany, 2009.

Kobus, H. (1980). Hydraulic modelling. Bulletin / DVWK 7, Paul Parey Verlag, Hamburg, Germany, 1980.

Schmidt, J., Wieland, J., Jensen, J., Findeisen, B., and Haufe, H. (2015a). “Hydraulischer Modellversuch Talsperre Malter – Herausforderungen infolge von schießendem Abfluss in gekrümmten Bauteilen.” *Proc., 38. Dresdner Wasserbaukolloquium „Messen und Überwachen im Wasserbau und am Gewässer“,* Dresdner Wasserbauliche Mitteilungen, Issue 53, Dresden, Germany, 109–118.

Schmidt, J., Wieland, J., and Jensen, J. (2015b). “Hydraulischer Modellversuch Talsperre Malter – Optimierung eines Teilungsbauwerkes mit vertikaler Strömungstrennung.” *Proc., 17. JuWi-Treffen*, Dresdner Wasserbauliche Mitteilungen, Issue 57, Dresden, Germany, 25–32.